2009

Developing a blood-mimicking fluid for particle image velocimetry with silicone vascular models

Majid Yacoub Yousif

Developing a blood-mimicking fluid for particle image velocimetry with silicone vascular models

(Spine title: A blood-mimicking fluid for vascular flow studies)
(Thesis format: Integrated-Article)

by

Majid Yacoub Yousif

Graduate Program in Biomedical Engineering

Submitted in partial fulfillment
of the requirements for the degree of
Master of Engineering Science

School of Graduate and Postdoctoral Studies
The University of Western Ontario
London, Ontario, Canada

Abstract

A new blood-mimicking fluid (BMF) has been developed which enables the study of flow in vascular models using particle image velocimetry (PIV).

PIV is a valuable engineering technique used to obtain accurate flow-related information, such as velocity and shear stress, in order to gain a better understanding of the hemodynamics related to the initiation and progression of vascular disease. In PIV, flow models are perfused with a fluid seeded with tiny particles. The distance traveled by particles over a specific time is measured, by correlating consecutive images from high resolution cameras, and used to determine fluid velocity. A major difficulty in PIV that affects measurement accuracy is the deflection and distortion of light passing through the model and the fluid, due to the difference in the refractive index (n) between the two materials. The problem can be eliminated by using a fluid with a refractive index matching that of the model. Such fluids are not commonly available, especially for vascular research where the fluid should also have a viscosity similar to human blood (4.4 ± 0.5 cP).

In this work, a new blood mimicking fluid (BMF) composed of varying relative concentrations of water, glycerol, and sodium iodide, has been developed to accommodate commonly used modeling materials such as silicone elastomers. The fluid exhibits a refractive index ranging between, but not limited to, 1.40 and 1.43 and a viscosity ranging between 4.16–4.69 cP. A mixture suitable for use with our silicone vascular models (Sylgard 184; $n = 1.414$) was produced by using relative concentrations (% by weight) of 47.38% water, 36.94% glycerol and 15.68% sodium iodide, with resulting viscosity of 4.31 ± 0.03 cP and refractive index of 1.4140 ± 0.0001.

This BMF enables PIV studies in vascular models of materials with various refractive indices while maintaining a suitable viscosity with respect to blood. Results demonstrating the possible range of refractive index and viscosity will be presented, as well as demonstrative digital particle images from flow in a carotid artery bifurcation flow model.

Keywords: blood-mimicking fluid, particle image velocimetry, refractive index, vascular model, silicone , Sylgard, viscosity, carotid bifurcation, elastomer

Contents

List of Tables

List of Figures

List of Acronyms & Abbreviations

2D	two-dimensional or two dimensions
3D	three-dimensional or three dimensions
BMF	blood-mimicking fluid
C	Celsius
cP	centipoise (a unit for dynamic viscosity)
cSt	centistokes (a unit for kinematic viscosity)
D	diameter (of a blood vessel or a pipe)
DUS	Doppler ultrasound
L	litre
P	Poise (a unit for dynamic viscosity)
DEP	diethyl phthalate
PIV	particle image velocimetry
Re	Reynolds number
US	ultrasound
vol.	volume
n	refractive index
μ	dynamic viscosity
ν	kinematic viscosity
ρ	density
u	fluid velocity
v	speed (e.g. light speed)

Chapter 1

Introduction

1.1 Motivation for this project

Ischemic stroke is a serious disease that causes high rates of mortality and morbidity throughout the globe. In fact, it is the third leading cause of death in Canada, where it contributes to about 6% (>14,000) of the annual deaths [1]. Ischemic stroke is caused by emboli, such as blood clots or bits of atherosclerotic plaque, which obstruct blood vessels and prevent adequate delivery of blood to affected regions of the brain. Such emboli are often known to develop at the bifurcation of the carotid artery where plaques of fat accumulate (Fig. 1.1). Plaque accumulation changes the vessel geometry and leads to stenosis (narrowing) in the vessel lumen. This induces changes to flow properties such as producing jet flow and turbulence, especially in severely stenosed vessels. Some flow conditions are believed to contribute to emboli formation, such as through plaque rupture and clot generation. Consequently, it is of interest to accurately study flow conditions in diseased carotid bifurcations.

A variety of techniques are used for flow studies *in vivo* and *in vitro*. Doppler ultrasound (DUS), for example, is used for both *in vitro* and *in vivo* flow analysis. For *in vitro* studies, laser Doppler velocimetry (LDV) can be used for obtaining quantitative flow information with high spatial resolution. With recent improvements, particle im-

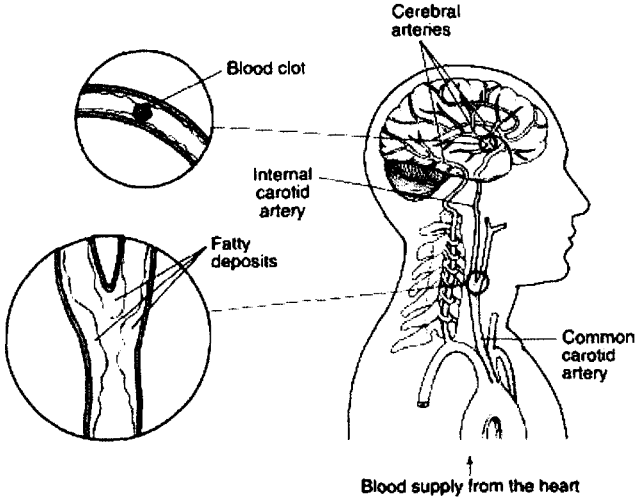

Fig. 1.1: The carotid artery bifurcation where plaque typically accumulates causing stenosis (narrowing) of the vessel lumen which can lead to changes in blood-flow parameters thus contributing to emboli formation and possibly subsequent ischemic stroke.

age velocimetry (PIV) has become a reference technique for quantitative flow studies because it has sufficiently high temporal and spatial resolution. PIV can conveniently provide detailed 2D velocity maps with two consecutive images, as opposed to tedious site-by-site acquisition required for LDV. Accordingly, PIV is used for different kinds of flow studies including comparison and evaluation of results obtained by other techniques. As a result, PIV is used as a part of a collaborative series of studies on flow parameters correlated with emboli formation and thus ischemic stroke. This work focuses on a major part of the PIV system, which is the blood-mimicking fluid required for vascular flow studies.

1.2 Particle image velocimetry (PIV)

1.2.1 Working principle

It is sometimes difficult to estimate the speed or the direction of a flowing river or stream, especially when the observer is not close enough to the site. However, if the water is carrying some tree leaves or any floating objects, the observer can more easily detect the flow direction and even give reasonable estimation of the stream velocity. The principle of particle image velocimetry was basically built on this simple idea.

In order to detect flow with a PIV system for vascular studies, the fluid is seeded with tiny particles (light scatterers) and images are taken using a camera with the help of a laser source of light. The tracer particles should be illuminated in the flow plane at least twice within a short time interval. The light reflected by the particles is then recorded on camera image frames from which the particles' displacements can be measured. It is important in most cases to apply specialized algorithms and sophisticated software to analyze the data recorded on PIV image frames. Applying correlation techniques enables tracking of the particles to detect the whole motion in a small region of interest. Accordingly, PIV has become widely used for flow studies in different applications such as aerodynamics, internal combustion engines, and vascular flow studies. The next section describes the major subsystems (units) of the PIV system used in our lab.

1.2.2 System components

As shown in Fig. 1.2, the PIV system consists of the following subsystems (units) which are further described in the following subsections:

1. Imaging unit

2. Pumping unit

3. Hydraulic model

4. Analysis software

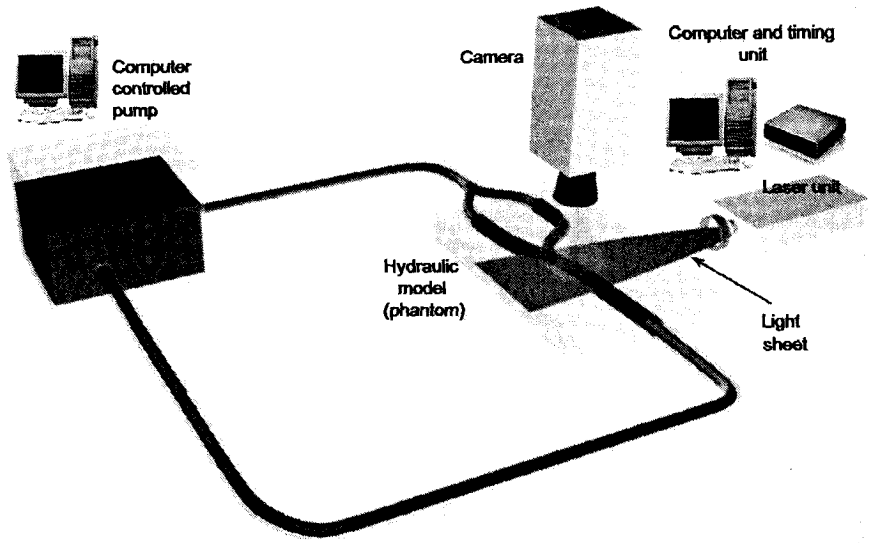

Fig. 1.2: A schematic of the PIV system showing the various components and subsystems. Modified based on Heise *et al.* [2][a].

1.2.2.1 Imaging unit

The imaging unit is mainly composed of the following parts:

- **Cameras**

  Two high speed high resolution digital (CMOS) cameras are used for image acquisition, with 1000 frames per second for full size resolution of 1024x1024

[a] The copyrights permission is shown in *Appendix A* of this thesis.

pixels, or up to 109,500 frames per second for reduced resolution.

- **Laser source**

  A laser sheet of light is used to illuminate the scatterers (particles) during the image acquisition process. The laser system used here is a 5.5 W diode-pumped Nd:YAG laser (LSR-532-TM-5000-10, LaserGlow.com Ltd., Toronto) with visible (green) light of a wavelength of 532 nm.

- **Sheet-forming optics**

  A set of optics to diverge the light beam into the required laser sheet needed to illuminate the particles within the field of interest.

- **Timing unit**

  The duration of the laser pulses and the timing between these pulses are controlled by the timing unit. This unit also controls the synchronization between the light pulses and the image acquisition process where the duration of a laser pulse may range between $13 - 2000$ μs, and the time between pulses can be set between $1.6 - 5000$ μs.

1.2.2.2 Pumping unit

- The pumping unit is composed of a computer-controlled pump (Compuflow, Shelly Medical Imaging). The pump generates the required flow rate and physiological waveform shape such as described by Holdsworth *et al.* [3]. The pump is controlled by a computer system with suitable software to set the flow parameters and produce the desired wave form.

1.2.2.3 Hydraulic model

The hydraulic model of our vascular studies is composed of the following parts:

- **Vascular flow phantom**

  A silicone (Sylgard 184, Dow Corning, Michigan, USA) phantom, incorporating a life-sized carotid bifurcation model, is used in this work with appropriate flow connectors as shown in Fig. 1.3. Silicone is a transparent material with a refractive index (n) ranging between 1.40–1.44 [7–10, 12]. Our phantoms are manufactured using a lost-metal casting method which enables modeling the desired dimensions and geometry with high accuracy.

- **Flow rig and tubing**

  This unit consists of a set of connectors and small-diameter tubing to mimic downstream vascular resistance and maintain flow under desired conditions such as physiological pressure [15].

1.2.2.4 Analysis software

- There is a computer unit equipped with specialized software (Davis 7.2, Lavision, Michigan, USA) to analyze the data acquired by the imaging system.

- The software is based on the cross-correlation algorithm to calculate the displacement of particles over time, from which velocity vector fields are produced.

1.2.3 PIV fluid properties

The fluid, suitable for our PIV system, should be transparent and colorless to minimize attenuation of the laser light in order to ensure optimal imaging conditions. The fluid should also be safe (i.e. non-toxic, non-flammable and non-reactive) and, ideally, available for a reasonable cost. These properties are usually part of the fluid features that cannot be modified. However, there are other, modifiable properties that are essential requirements of the PIV fluid used in this work. In particular, refractive index and viscosity, which are further discussed below, are both important parameters

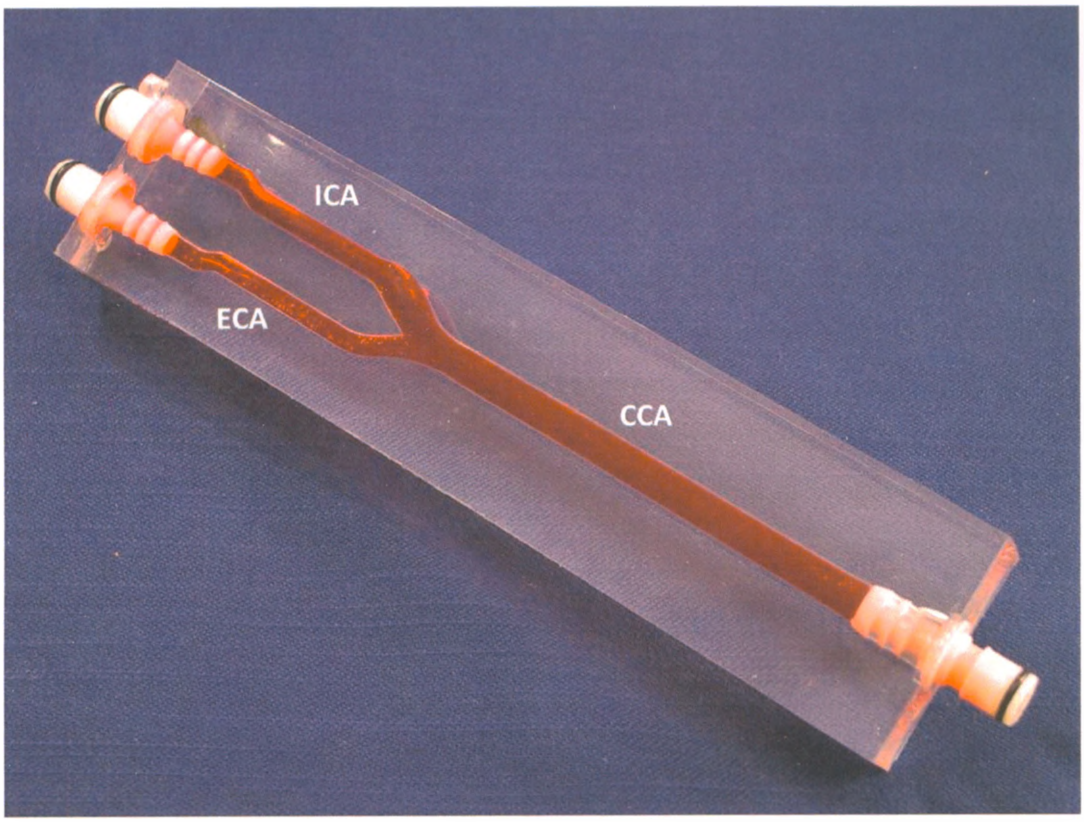

Fig. 1.3: A silicone (Sylgard 184) phantom representing a normal (disease-free) model of the carotid bifurcation. The model shows the common carotid artery (CCA) branching into the internal carotid artery (ICA) and the external carotid artery (ECA), with realistic diameters of 8.0 mm, 5.52 mm and 4.62 mm, respectively. Plastic coupling connectors are used at both ends of the phantom for quick connection.

to be satisfied in the PIV fluid used for our system. It is important to mention here that adequate fluids for performing vascular research with this PIV system, are not naturally available. Consequently, two or more fluids, or material components, should be mixed together to achieve the target refractive index and viscosity, on top of the typical, non-modifiable properties.

1.2.3.1 Refractive index (n)

Light travels at a constant speed within a uniform medium [16]. When a light ray (incident) in a particular medium, travels through an interface to an adjacent medium, the ray changes its path and travels with a new angle named the angle of refraction (Fig. 1.4A). This is caused by the difference in light speed within each medium. The ratio of light speed in vacuum (c) to the light speed in the given medium (v) is named the refractive index (or index of refraction, $n = \frac{c}{v}$) of that medium.

Snell's law introduces the following relation for an incident light beam and a refracted light beam when light passes through the interface between two media:

$$n_1 \sin\theta_1 = n_2 \sin\theta_2 \tag{1.1}$$

From this law and the refractive index formula ($n = \frac{c}{v}$), a general form for refraction is derived as follows:

$$\frac{\sin\theta_1}{\sin\theta_2} = \frac{v_1}{v_2} = \frac{n_2}{n_1} \tag{1.2}$$

where:

θ_1 is the angle of incidence within the first medium relative to the normal at the interface;

θ_2 is the angle of refraction into the second medium (refracted angle of transmission), as shown in Fig. 1.4;

v_1 and v_2 represent the light speeds in the two media;

n_1 and n_2 are the refractive indices of the two media (materials) respectively;

Refraction causes apparent optical distortion of objects within one medium (such as water) when observed from another adjacent medium (such as air) [16]. When refraction occurs in an optical system such as PIV, it causes distorted images thus affecting the measurement accuracy. In order to avoid refraction problems, the refractive index of a PIV fluid should be matched to that of the phantom, otherwise

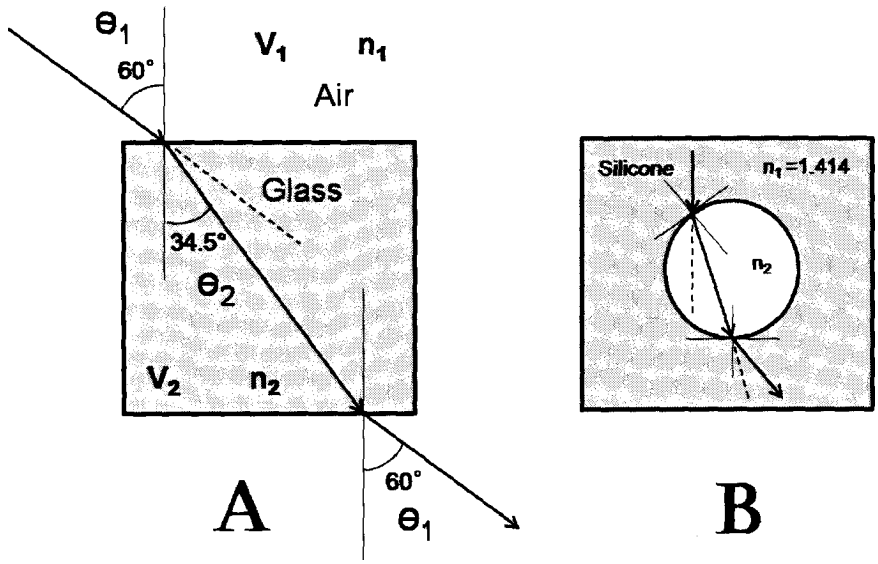

Fig. 1.4: (A) Refraction occurs when light travels through an interface between different media, such as air and glass where light has different speeds (v_{air} and v_{glass}) *or* (v_1 and v_2) respectively, therefore a light beam changes its original direction (broken line) and travels along the path indicated by the arrow inside the glass. (B) A schematic representing a cross section in a silicone phantom with a circular vessel lumen. When the lumen contains a fluid with a refractive index (n_2) that is different from silicone, light will refract and change its original direction (broken line), traveling along the path indicated by the arrow inside the fluid. In the given example, the fluid has a refractive index higher than that of silicone ($n_2 > n_1$).

distorted images and inaccurate flow information may be acquired, especially from within flow channels with curved surfaces [17] such as a circular blood-vessel lumen (Fig. 1.4B).

Since our phantoms are manufactured from Sylgard 184, our PIV fluid should have a refractive index matching that of Sylgard 184. Unfortunately, the index of refraction for silicone elastomers is cited in the literature as having values between 1.40–1.44 [7–10, 12], and also for Sylgard 184 where the cited value varies between 1.41–1.43 even by the same supplier of the material [8, 9, 13, 14]. Moreover, the silicone refractive index might exhibit batch-to-batch (i.e. phantom-to-phantom) variability because

silicone usually comes into two liquid forms that are mixed together and allowed to cure in order to produce the final homogeneous material. Accordingly, such variances in refractive index may severely affect the PIV measurements because distortion seen in images is very sensitive to small difference in refractive indices, even beyond the third decimal digit. This implies the need to adjust a specific formulation of blood mimicking fluid to work for each particular phantom. The main goal of this thesis was to develop a blood-mimicking fluid that is adjustable to match the refractive indices of different silicone phantoms.

1.2.3.2 Viscosity

Viscosity, an inherent fluid property, is a major flow determinant. Most mathematical flow models, such as Poiseuille's formula (Equation 1.3) and Reynolds number (Equation 1.4), include viscosity as an important flow parameter. As shown in the Poiseuille equation below, the fluid viscosity (μ) represents an important factor that affects the resulting flow rate (Q) for the a given pressure drop (ΔP) over a distance (L) in a vessel with a diameter (D):

$$Q = \frac{\pi D^4 \Delta P}{128 \mu L} \tag{1.3}$$

Also, as Reynolds number (Re) suggests, fluid flow can be described based on two major components, namely inertial forces and viscous forces, as shown in the following formula:

$$Re = \frac{\rho u D}{\mu} = \frac{u D}{\nu} = \frac{inertial forces}{viscous forces} \tag{1.4}$$

where:

Re is Reynolds number (unitless),

D is the vessel diameter (cm),

u is the mean velocity of the flowing fluid (cm/s),

μ is the dynamic viscosity (Poise, P)(1 P = 1 g/cm·s), given $\mu = \nu\,\rho$

ν is the kinematic viscosity of the fluid (Stokes, St)(1 St = 1 cm^2/s), and

ρ is the fluid density (g/cm^3).

In order to accurately replicate the *in vivo* flow conditions, the PIV fluid should mimic human blood viscosity for the types of flow being studied. A comprehensive literature search of recent studies, suggested a value of 4.4 ± 0.5 cP for human blood viscosity at high shear rates, as shown in Table 1.1.

Table 1.1: Dynamic viscosity of human blood based on recent studies on normal controls. References are listed in approximated increasing order of dynamic viscosity (μ) in order to more clearly show the range of values.

Reference	**Dynamic Viscosity (cP) Mean ± STD** [a]	**Shear Rate** (s^{-1})	**Notes**
Vaya *et al.* (2008) [24]	3.93±0.48	230	
Galduroz *et al.* (2007) [25]	3.37±0.3	250	Females (18-60 years)
	3.79±0.09	250	Males (18-60 years)
	4.19±0.3	250	Males (over 60 years)
	4.36±0.3	250	Females (over 60 years)
Carrera *et al.* (2008) [26]	3.74±0.48	230	High shear rate
	4.06±0.55	115	Low shear rate
Rajzer *et al.* (2007) [27]	4.3±0.9	100-400	
Kucukatay *et al.* (2007) [28]	4.84±0.34	150	
Fehr *et al.* (2008) [29]			Hours after drinking water:
	4.90±0.12	94.5	0 hours
	4.91±0.10	94.5	1 hour
	4.91±0.17	94.5	2 hours
	4.95±0.13	94.5	4 hours
	4.97±0.15	94.5	13 hours
Mean ± STD	**4.4±0.5**		

[a] Standard Deviation

The condition of viscosity is not properly addressed in the PIV literature where most references tend to satisfy only the refractive-index requirement. Table 1.2 gives

a summary of some studies that consider working with the resulting viscosity after matching the refractive index, even if the viscosity is not close to human blood, whereas other references apply scaling methods to compensate for the difference in viscosity. In brief, no previous work in the literature introduces a blood-mimicking fluid that works for silicone phantoms while satisfying both refractive index and viscosity, simultaneously. Furthermore, both refractive index and viscosity are temperature dependent, therefore it is necessary to satisfy both properties at the same temperature, which adds further difficulties. A fluid formulation is introduced in this work with a range of refractive indices matching most common silicone elastomers, and with corresponding viscosity values within the range of human blood (4.4 ± 0.5 cP).

1.3 Blood mimicking fluids in the literature

Many PIV fluids are introduced in the literature as blood-mimicking fluids for vascular research. Table 1.2 gives a summary of the most commonly used fluids in PIV vascular research. In particular, the following three major categories are apparent: water-glycerol based fluids, sodium iodide based fluids, and ethanol-DEP (diethyl phthalate) based fluids. Various other fluids, such as dibutyl phthalate [7] and potassium thiocyanate, have been described in the literature, but are not very common and have the least usage. Potassium thiocyanate, for example, has been found to be highly corrosive to metal components in the system, such as some pump parts.

As shown in Table 1.2, the fluids commonly in use are designed for different hydraulic model materials such as glass, acrylic and silicone. The table also includes all available viscosity data, as well as other notes on each formulation.

Although Table 1.2 exhibits many fluid formulations, none demonstrates a simultaneous match for refractive index and viscosity to work with silicone phantoms in vascular research. A detailed description about the pros and cons of the three major

Table 1.2: Blood-mimicking fluids described in the literature for use with different hydraulic models. Note that n is the refractive index, μ is the dynamic viscosity, ν is the kinematic viscosity and ρ is the density of the fluid.

Reference	Fluid components (by volume)	n	μ (cP)	ν (cSt)	ρ (g/ml)	Notes
Water-glycerol based fluids						
Brunette *et al.* (2008) [14]	37% water 63% glycerol	1.43	14.5	N/A	N/A	**Silicone** phantoms of coronary artery.
Heise *et al.* (2005) [2]	58% water 42% glycerol	N/A	4.0	N/A	N/A	**Silastic**® models for flow studies at peripheral bypasses.
Lim *et al.* (2001) [20]	64% water 36% glycerol	N/A	3.5	3.46[b]	1.01	Flow studies of aortic valve. *Refractive-index not matched.*
Yip *et al.* (2004) [9]	57% water 43% glycerol	1.414	N/A	N/A	N/A	Aortic model from **silicone** (Sylgard 184) at 25 °C. *"No attempt was made to match the viscosity of blood"* [9].
Sodium-iodide based fluids						
Browne *et al.* (2000) [18]	79% sodium iodide 20% glycerol 1% water	1.49	5.95[b]	3.5	1.47[a]	**Acrylic** chamber representing the aortic root.
Fontaine *et al.* (1996) [5]	79% sodium iodide 20% glycerol 1% water	1.49	5.95[b]	3.5	1.47	**Acrylic** mechanical aortic valve.
Lenssen *et al.* [19]	50% sodium iodide 15.5% glycerol 34.37% water 0.03% xanthan gum	1.49	N/A	N/A	N/A	**Acrylic** vascular models. *No information on viscosity provided.*
Liou *et al.* (1997) [21]	60% sodium iodide (by weight) in water	N/A	2.54	1.46[b]	1.73	Laser Doppler velocimetry in **Pyrex**® aneurysm models.
Sankovic *et al.* (2004) [22]	sodium iodide water	1.485	5.4[b]	3.2	1.69	**Acrylic** model of a rotary blood pump.
DEP[c]*-ethanol based fluids*						
Nguyen *et al.* (2004) [7]	55.6% DEP 44.4% ethanol	1.44	3.35[b]	3.327	1.007[b]	**Silicone** models at 16.9 °C.
Miller *et al.* (2006) [10]	36.3% DEP 63.7% ethanol	1.41	1.8	N/A	N/A	**Silicone elastomer**
	70.3% DEP 29.7% ethanol	1.4585	3.499	N/A	N/A	**Fused quartz**
	81.1% DEP 18.9% ethanol	1.474	4.86	N/A	N/A	**Pyrex glass** Results based on empirical model introduced by [7].
Other fluids						
Day *et al.* (2005) [4]	100% dibutyl-phthalate	1.485	5.0	4.76[b]	1.05	**Acrylic** model of centrifugal blood pump. Fluid properties attained at 50 °C.

[a] As given by Fontaine *et al.* [5] for the same fluid composition and percentage ratios

[b] Value calculated based on given information

[c] Diethyl phthalate

fluids (water-glycerol, water-glycerol-sodium iodide, and diethyl phthalate-ethanol) is given below to better clarify the implications of the new fluid formulation developed in this work.

1. **Water-glycerol solution**

   This is the most commonly used fluid in vascular research. However, the fluid does not satisfy all requirements for working with silicone elastomers. In preliminary work, formulations with different glycerol content ($52-59\%$ by volume) were investigated at different temperatures ($22-28\,^{\circ}\mathrm{C}$). Although the resulting formulations achieved a match of refractive index to our Sylgard-184 phantoms, all corresponding viscosity values were higher than human blood. Following are the major pros and cons of the water-glycerol solution for PIV:

   <u>Pros</u>

   - Transparent and colorless;
   - Safe: non-flammable, non-toxic and non-reactive;
   - Modifiable: where different formulations can be developed by changing the relative concentrations of water and glycerol to match a wide range of refractive indices with different viscosity values;
   - Cost: available under reasonable cost (one litre of glycerol costs around $13);

   <u>Cons</u>

   - High viscosity: most formulations with matching refractive indices to common silicone elastomers ($n = 1.40$–1.44) have viscosity values much higher than human blood ($\mu = 4.4 \pm 0.5$ cP). This is caused by the very high viscosity of glycerol ($\mu_{glycerol} = 1490$ cP at $20\,^{\circ}\mathrm{C}$) [33], which means small increments of glycerol content will produce large changes in the viscosity of the resulting fluid. As shown in Table 1.3, a fluid with a refractive

index around 1.40 (the lower bound of silicone elastomers) would have a dynamic viscosity of 6.0 cP which is higher than the acceptable range of human blood viscosity (4.4 ± 0.5 cP). Accordingly, higher viscosity values are expected for fluids with refractive index above 1.40. On the other hand, a water-glycerol formulation that demonstrates a viscosity similar to blood should contain around 40% (by volume) of glycerol, based on Table 1.3. Such fluid would have a refractive index less than 1.40, therefore it cannot achieve a match with any silicone elastomer (n = 1.40–1.44). As a result, this fluid formulation fails to work as a blood-mimicking fluid for silicone phantoms.

Table 1.3: Water-glycerol refractive index and dynamic viscosity at 20 °C as given by [32].

Glycerol in Solution (% by weight)	Glycerol in Solution (% by vol.) [a]	Dynamic viscosity μ (cP)	Refractive index (n)
30	25.4	2.50	1.37070
40	34.6	3.72	1.38413
50	44.2	6.00	1.39809
60	54.3	10.80	1.41299
65	59.6	15.20	1.42044
70	64.9	22.50	1.42789
75	70.4	35.50	1.43534
80	76.0	60.10	1.44290
100	100	1490 [33]	1.47399

[a] Values in this column were calculated from column 1 (glycerol in solution by weight), considering a glycerol density of 1.261 g/cm^3

2. **Sodium iodide solutions**

This formulation is introduced by many references in the literature but mainly for hydraulic models fabricated from glass (n = 1.474–1.520) and acrylic (n = 1.485–1.492). As shown in Table 1.2, some references use a combination of sodium iodide and water [22], whereas others add glycerol to the combination [5, 18]. However, both formulations demonstrate relatively high refractive indices

within the range of glass and acrylic. The following major pros and cons are considered for sodium-iodide based fluids:

Pros

- Transparent and colorless;
- Safe: non-flammable, non-toxic and non-reactive;
- Cost: available for a reasonable cost (one litre of the fluid costs between \$20–\$30);

Cons

- High refractive index: as the previously targeted refractive index values for acrylic (n = 1.485–1.492) and glass (n = 1.474–1.520) are higher than silicone elastomers (n = 1.40–1.44);
- High dynamic viscosity: where the corresponding dynamic viscosity values (>5.4 cP) are higher than that of human blood (4.4 ± 0.5 cP);
- Instability: this formulation suffers a discoloration problem caused by the iodide ion (I^{3-}) which is released in water, changing the colorless fluid to yellow. However, this problem is reversible by adding 0.1% (by weight) sodium thiosulphate [31]. Moreover, one can avoid the yellowing problem by adding the sodium thiosulphate when mixing the initial components to generate the formulation;

3. **Diethyl-phthalate (DEP) and ethanol solution**

This formulation is introduced by Nguyen *et al.* [7] with an empirical model that makes it possible to match different refractive index values at different temperatures. In preliminary work, the model was applied to investigate the refractive index for all silicone elastomers (1.40 - 1.44) as well as the corresponding viscosity values, at different working temperatures ($19 - 34\,^{\circ}C$). Although it was

possible to characterize different formulations for the target range of refractive index, all the corresponding viscosity values were below the range of human blood. For example, at 24 °C, refractive index values between 1.40 and 1.44 can be achieved with ethanol content of 70.5% to 42.5% respectively, whereas at 29 °C the concentration of ethanol in solution is between 69% and 41% respectively. Based on the model, the maximum attainable viscosity values were for formulations with a refractive index of 1.44, which corresponded to 2.8 cP at 24 °C and 2.6 cP at 29 °C. Such values are clearly below the range of human blood viscosity (4.4 ± 0.5 cP). Following are the major pros and cons of the DEP-ethanol solution:

Pros

- Transparent and colorless;
- Covers a wide range of refractive index values;
- Stability: the formulation is insensitive to light exposure therefore is considered to be more stable than other fluids that are light sensitive;
- Availability: both DEP and ethanol are available under reasonable cost where one litre of the formulation may cost between $\$18 - \$25$ based on the DEP content in the formulation. Note that one litre of DEP costs approximately \$27 whereas a litre of ethanol costs only \$8;

Cons

- Refractive index and viscosity are coupled, where formulations with high refractive index might demonstrate acceptable viscosity for blood whereas formulations with lower refractive index, suffer lower viscosity. The refractive index for silicone elastomers ranges between 1.40–1.44, which is successfully attainable by using a percentage of DEP in solution between 36.3%-55.6%, based on Nguyen's model [7]. However, the resulting viscos-

ity for such concentration of DEP would lie between 1.8–3.3 cP, if cooled to a relatively low temperature of 16.9 °C. Such viscosity values are still below the lowest bound of human blood viscosity (3.9 cP) based on 4.4 ± 0.5 cP given in Table 1.1;

- High flammability: due to ethanol component;
- Instability: ethanol is known to have high volatility which leads to rapid and significant evaporation, resulting in changes in refractive index and viscosity of the formulation. Accordingly, a tightly sealed system is required in order to work with this formulation;
- Temperature instability: where the dynamic viscosity of the fluid is sensitive to temperature, particularly for formulations with high DEP concentration;

1.4 Hypothesis

The hypothesis of this thesis is that it is possible to produce a PIV blood-mimicking fluid that simultaneously demonstrates a dynamic viscosity similar to human blood (4.4 ± 0.5 cP) and a refractive index appropriate for silicone-elastomer phantoms (n = 1.40–1.44), by controlling the relative composition ratios of a three-component fluid composed of water, glycerol, and sodium iodide salt.

1.5 Research objectives

The research objectives of this thesis are the following:

1. Determine the refractive index of custom-moulded silicone phantoms used for vascular research;

2. Formulate a PIV fluid with an appropriate viscosity that matches with human blood, while simultaneously matching the refractive index of the vascular silicone-elastomer phantom;

3. Characterization of different formulations of the PIV fluid to achieve different ranges of refractive index and viscosity values in order to accommodate variances in refractive index from phantom to phantom;

1.6 Thesis outline

1.6.1 Chapter 1:

Chapter 1 presents the clinical motivation and background work, particularly literature search results.

1.6.2 Chapter 2:

This chapter describes the development and characterization of a blood-mimicking fluid based on the aforementioned research objectives. A version of chapter 2 has been submitted to the peer-reviewed journal Experiments in Fluids.

1.6.3 Chapter 3:

This chapter gives a summary of the work done in this thesis as well as the future directions of the research.

References

[1] The Heart and Stroke Foundation, Statistics, *www.heartandstroke.com/site/c.ikIQLcMWJtE/b.3483991/k.34A8/Statistics.htm*

[2] M. Heise, U. Kruger, R. Ruckert, R. Pfitzman, P. Neuhaus and U. Settmacher, "Correlation of intimal hyperplasia development and shear stress distribution at the distal end-side-anastomosis, in vitro study using particle image velocimetry", *Eur J Vasc Endovasc Surg* , vol. 26, pp. 357–366, 2003.

[3] D. W. Holdsworth, D. W. Rickey, M. Drangova, D. J. M. Miller, A. Fenster, " Computer-controlled positive displacement pump for physiological flow simulation", *Med. & Bio. Eng. & Comput.*, vol. 29, pp. 565–570, 1991.

[4] S. W. Day and J. C. McDaniel, "PIV measurements of flow in a centrifugal blood pump: steady flow", *Transactions of the ASME*, vol. 127, pp. 244-253, 2005.

[5] A. A. Fontaine, J. T. Ellis, T. M. Healy et al, "Identification of peak stresses in cardiac prostheses - A comparison of two-dimensional versus three-dimensional principal stress analyses", *ASAIO Journal*, vol. 42, pp. 154–163, 1996.

[6] T. Yagi, W. Yang, D. Ishikawa, H. Sudol, K. Iwasaki, and M. Umezul, "Multiplane scanning stereo-PIV measurements of flow inside a spiral vortex pulsatile blood pump", *In: 13th Int Symp on Applications of Laser Techniques to Fluid Mechanics*, Lisbon, Portugal, 2006.

[7] T. T. Nguyen, Y. Biadillah, R. Mongrain, J. Brunette, J.-C. Tardif, and O. F. Bertrand, "A method for matching the refractive index and kinematic viscosity of a blood analog for flow visualization in hydraulic cardiovascular models", *Journal of Biomechanical Engineering*, vol. 126, pp. 529–535, 2004.

[8] L. M. Hopkins, J. T. Kelly, A. S. Wexler, and A. K. Prasad, "Particle image

velocimetry measurements in complex geometries", *Experiments in Fluids*, vol. 29, pp. 91–95, 2000.

[9] R. Yip, R. Mongrain , A. Ranga, J. Brunette, and R. Cartier, "Development of anatomically correct mock-ups of the aorta for PIV investigations", *Canadian Design Engineering Network CDEN Conference*, Montreal, 2004.

[10] P. Miller, K. Danielson, G. Moody, A. Slifka, E. Drexler, and J. Hertzberg, "Matching index of refraction using a diethyl phthalate/ethanol solution for in vitro cardiovascular models", *Experiments in Fluids*, vol. 41, pp. 375–381, 2006.

[11] A. Giambattista, B. Richardson, and R. C. Richardson, "College Physics Book", *McGraw Hill Higher Education*, pp. 840–846, 2004.

[12] K. Nishino, and J.-W. Choi, "Index-matching PIV for complex flow geometry", *4th Japan-Korea Joint Seminar on Particle Image Velocimetry*, Sept. 29-Oct.1, Kobe, Japan, 2006.

[13] P. Peterka, I. Kak, V. Matejec, J. Kanka, M. Karsek, M. Hayer and J. Slnicka, "Novel coupling element for end-pumping of double-clad fibres", *ECOC.*, We4.P.127, pp. 25–29, 2005.

[14] J. Brunette, R. Mongrain, J. Laurier, R. Galaz, and J. C. Tardif, "3D flow study in a mildly stenotic coronary artery phantom using a whole volume PIV method", *Med Eng Phys*, vol. 30, pp. 1193–1200, 2008.

[15] T. L. Poepping, H. N. Nikolov, R. N. Rankin, M. Lee, and D. W. Holdsworth, "An in-vitro system for Doppler ultrasound flow studies in the stenosed carotid artery bifurcation", *Ultrasound Med Biol*, vol. 28, pp. 495–506, 2002.

[16] P. E. Tippens, "Physics", Textbook, *McGraw Hill*, seventh edition, pp. 678, 2207.

[17] R. Budwig, "Refractive index matching methods for liquid flow investigations", *Experiments in Fluids*, vol. 17, pp. 350–355, 1994.

[18] P. Browne, A. Ramutaz, R. Saxena, and A. P. Yoganathan, "Experimental investigation of the steady flow downstream of the St. Jude bileaflet heart valve: A comparison between laser Doppler velocimetry and particle image velocimetry techniques", *Annals of Biomedical Engineering*, vol. 28, pp. 39–47, 2000.

[19] A. M. Lenssen, "A comparison between the influence of Bjork-Shiley monostrut and Carbomedics mechanical heart valves in the 50cc Penn State LVAD (V2) using PIV", *Pennsylvania State University*, Supervisors: Prof. Dr. Ir. F. N. vd. Vosse and Dr. K. B. Manning.

[20] W. L. Lim, Y. T. Chew, T. C. Chew, and H. T. Low, "Pulsatile flow studies of a porcine bioprosthetic aortic valve in vitro: PIV measurements and shear-induced blood damage", *Journal of Biomechanics*, vol. 34, pp. 1417-1427, 2001.

[21] T.-M. Liou, W.-C. Chang, and C.-C. Liao, "LDV measurements in lateral model aneurysms of various sizes", *Experiments in Fluids*, vol. 23, pp. 317–324, 1997.

[22] J. M. Sankovic, J. R. Kadambi, M. Mehta, W. A. Smith, and M. P. Wernet, "PIV investigations of the flow field in the volute of a rotary blood pump", *Journal of Fluids Engineering-Transactions of the Asme*, vol. 126, pp. 730–744, 2004.

[23] S. Raz, S. Einav, Y. Alemu, and D. Bluestein, "DPIV prediction of flow induced platelet activation–comparison to numerical predictions", *Annals of Biomedical Engineering*, DOI: 10.1007/s10439–007–9257–2, 2007.

[24] A. Vaya, J. Murado, M. Santaolaria, M. Simo, and L. Mico, "Haemorheological changes in patients with systemic lupus erythematosus do not seem to be related to thrombotic events", *Clinical Hemorheology and Microcirculation*, vol. 38, pp. 23-29, 2008.

[25] J. C. F. Galduroz, H. K. Antunes, and R. F. Santos, "Gender- and age-related variations in blood viscosity in normal volunteers: A study of the effects of extract of Allium sativum and Ginkgo biloba", *Phytomedicine*, vol. 14, pp. 447-451, 2007.

[26] L. Carrera, R. Etchepare, M. Arrigo, S. Vaira, J. Valverde, A. D'Ottavio and P. Foresto, "Hemorheologic changes in type 2 diabetic patients with microangiopathic skin lesions. A linear discriminant categorizing analysis", *Journal of Diabetes and Its Complications*, vol. 22, pp. 132-136, 2008.

[27] M. W. Rajzer, M. Klocek, W. Wojciechowska, I. Palka, and K. L. Kawecka-Jaszcz, "Relationship between, blood viscosity, shear stress and arterial stiffness in patients with arterial hypertension", *Elsevier B.V.*, 2007.

[28] M. Bor-Kucukatay, A. Keskin, H. Akdam, S. Kabukcu-Hacioglu, G. Erken, P. Atsak, and V. Kucukatay, "Effect of thrombocytapheresis on blood rheology in healthy donors: Role of nitric oxide", *Transfusion and Apheresis Science*, doi:10.1016/j.transci, 2008.

[29] M. Fehr, K. S. Galliard-Grigioni, and W. H. Reinhart, "Influence of acute alcohol exposure on hemorheological parameters and platelet function in vivo and in vitro", *Clinical Hemorheology and Microcirculation* , vol. 39, pp. 351-358, 2008.

[30] N. Antonova, E. Zvetkova, I. Ivanov and Y. Savov, "Hemorheological changes and characteristic parameters derived from whole blood viscometry in chronic heroin addicts", *Clinical Hemorheology and Microcirculation* , vol. 39, pp. 53-61, 2008.

[31] T. L. Narrow, M. Yoda, and S. I. Abdel-Khalik, "A simple model for the refractive index of sodium iodide aqueous solutions", *Experiments in Fluids*, vol. 28, pp. 282-283, 2000.

[32] The Dow Chemical Company, "Refractive Index and dynamic viscosity of Glycerine-Water Solutions at 20 °C", (1965–2009).

[33] R. C. Weast, "CRC handbook of chemistry and physics. A ready-reference book of chemical and physics data", *Chemical Rubber Company*, CRC Press, Clevelend, Ohio, USA, 1969.

Chapter 2

A new blood-mimicking fluid for particle image velocimetry with silicone vascular models

The content of this chapter has been adapted from: "A new blood-mimicking fluid for particle image velocimetry with silicone vascular models", submitted for publication to Experiments in Fluids, by Majid Y. Yousif, David W. Holdsworth, and Tamie L. Poepping.

2.1 Introduction

Particle image velocimetry (PIV) is an optical technique used to obtain quantitative flow information. The flowing fluid is seeded with tiny particles (i.e. light scatterers), and a pulsed laser sheet of light is used to illuminate these particles. Images are taken, using a high-resolution camera, in consecutive time intervals synchronized with the laser pulses. The images are analyzed with correlation algorithms to determine the distances traveled by particles, from which velocity vectors are then calculated.

To use PIV for vascular research, blood vessels are modeled in transparent phantoms fabricated from different materials, such as glass (refractive index, n = 1.474–1.520), acrylic (n = 1.485–1.492), and silicone (n = 1.40–1.44) [1–4, 6] . The latter is of particular interest due to its versatility and robustness: silicone is readily available in a two-part liquid form that makes it easy to cast into the required geometry and dimensions with high accuracy. Accordingly, silicone was used in this work to cast anthropomorphic phantoms of vascular models (Fig. 2.1) for studying hemodynamics at the bifurcation of the common carotid artery. In particular, the carotid models, based on in vivo geometric characterization [7], were manufactured using a lost-material casting technique [8, 9].

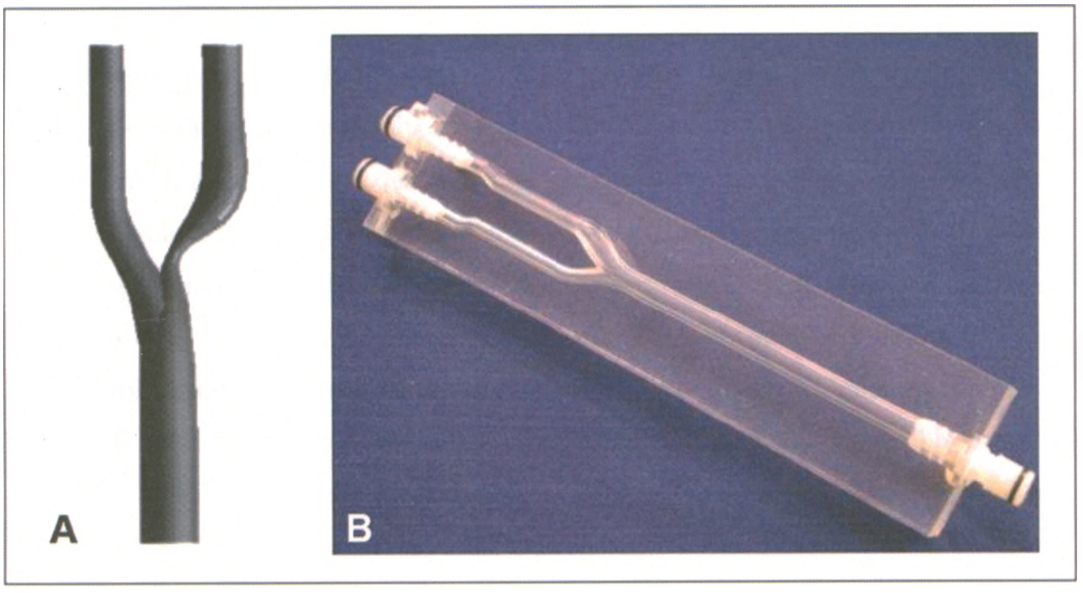

Fig. 2.1: (A) Example of a common carotid artery bifurcation model with severe (70%) eccentric (i.e. asymmetric) stenosis of the internal carotid artery branch (shown branching to the right), which leads to the brain. (B) Example of a silicone flow phantom, such as used in our PIV experiments, incorporating a different (normal, disease-free) carotid model.

Imaging with PIV requires a match of refractive index between the transparent

model and the flowing fluid in order to eliminate optical problems caused by refraction. Accordingly, it has been a major objective of any PIV fluid to exhibit a refractive index matched accurately to that of the phantom, where the refractive index of the phantom is not always known *a priori* and can vary for a given material. For example, the refractive index of Sylgard 184 (Dow Corning, Michigan, USA) as quoted in the literature, varies between 1.41 and 1.43 [1, 10]. Moreover, in vascular research, the PIV fluid should mimic human blood with respect to dynamic viscosity (μ) so as to obtain realistic blood-flow modeling measurements. Also, since the refractive index and viscosity are known to be temperature dependent, it is important to attain both properties at the same working temperature. Unfortunately, a blood-mimicking fluid (BMF) that demonstrates a refractive index matching with silicone and a dynamic viscosity similar to blood, both at the same temperature and preferably room temperature, is not readily described in the literature.

A blood analogue commonly used in the literature is a composition of glycerol and water [2, 11, 12], which demonstrates good optical properties as well as safety, availability, and compatibility with silicone models. However, this fluid fails to satisfy the refractive index and viscosity requirements simultaneously. Because viscosity and refractive index are similarly correlated with the glycerol concentration, an increase in glycerol simultaneously increases both viscosity and refractive index. Attaining a refractive index value greater than 1.40 requires greater than 40% glycerol by volume and thus a resulting viscosity greater than 5.0 cP. For example, a composition of 36.6% (by vol.) glycerol in water would demonstrate a dynamic viscosity around 3.5 cP, which closely approximates that of blood [2, 11, 12], but the resulting refractive index of 1.38 is lower than the refractive index of commonly used silicone elastomers ($n = 1.40$–1.44). A composition of 63% (by vol.) of glycerol in water has been shown to have a refractive index of 1.43, providing a match with some silicone elastomers, but with a rather high dynamic viscosity of 14.5 cP [13]. Such dynamic viscosity is notably higher than the range of human blood (4.4 ± 0.5 cP) found in the literature

as summarized in Table 1.1.

Another fluid, with an empirical model introduced by Nguyen *et al.* [2], suggests combinations of diethyl phthalate (DEP) and ethanol for a BMF with a wide range of refractive index and viscosity values at different temperatures. The model shows good results for matching the refractive index to various silicone elastomers using different percentages of the DEP and ethanol at different temperatures including room temperature ($20 - 25\,^{\circ}\mathrm{C}$). However, the resulting viscosity values were lower than human-blood viscosity. As shown experimentally [2], the fluid model produces a kinematic viscosity of 3.327 cSt (corresponding to a dynamic viscosity of approximately 3.3 cP) by mixing 55.6% (by vol.) DEP and 44.4% (by vol.) ethanol, which corresponds to a refractive index of 1.44 at $16.9\,^{\circ}\mathrm{C}$. Such viscosity lies well outside the lower bound of human blood viscosity (3.9 cP) based on Table 1.1. In addition, the model suggests lowering the relative amount of DEP to obtain fluids with refractive indices below 1.44 for matching other elastomers (i.e. silicones with n between 1.40 and 1.44). However, this will further decrease the resulting viscosity of the BMF since the DEP represents the more viscous component, with a viscosity about ten times that of the ethanol [2]. Accordingly, the expected viscosity values for fluids with refractive indices matching to silicone elastomers will be well below an acceptable level for human blood. Note that the empirical model also suggests a relatively low temperature ($16.9\,^{\circ}\mathrm{C}$) to achieve the proposed viscosity, which requires a temperature-control system. In addition, this fluid suffers a significant change in refractive index and dynamic viscosity when left uncovered in a well-ventilated room [3], due to the rapid evaporation of ethanol from the solution, and thus one requires a closed system as a condition to work with the fluid.

Another BMF composed of different percentages of water, glycerol and sodium iodide was also introduced in the literature for use with models fabricated from acrylic (n = 1.485–1.492) [14, 16–18]. Such refractive index values are much higher than commonly known silicone elastomers (n = 1.40–1.44), therefore these formulations

cannot be directly applied to silicone models. Moreover, the resulting viscosity values, although close, are still higher than human blood viscosity found in the literature (4.4 ± 0.5 cP). For example, Yagi et al. [18] mentions a kinematic viscosity of 3.3 cSt which corresponds to a dynamic viscosity of 5.61 cP based on the given fluid density (1.7 g/mL). The calculated dynamic viscosity for the formulation introduced by Sankovic *et al.* [16] was 5.4 cP based on a 3.2 cSt kinematic viscosity with a fluid density of 1.69 g/mL. Accordingly, these formulations have both refractive index and viscosity values that are higher than our targeted values.

Consequently, the various PIV fluids of previous work mentioned in the literature demonstrate either a match of refractive index with silicone models or a viscosity close to blood, but none demonstrates a simultaneous match of the two properties. This paper introduces a method for developing a blood-mimicking fluid for use at room temperature with a range of refractive indices matching to most commonly used silicone elastomers while simultaneously exhibiting acceptable dynamic viscosity that mimics human blood. The method proposed here is based on controlling the relative composition percentages of water, glycerol, and sodium iodide in solution. The formulation can be adjusted while monitoring the refractive index match to the phantom *via* the elimination of optical distortion; in this way, the refractive index of a given phantom material can be accurately matched, and thus it then can also be accurately determined by measuring the fluid's refractive index using a refractometer.

2.2 Materials and methods

2.2.1 Flow loop for measuring the refractive index of the phantom

Sylgard-184 silicone is specified in the literature with refractive index values ranging between 1.41–1.43 [1, 4, 10, 13]. In addition, the refractive index may vary from

batch to batch (i.e. phantom to phantom). We aim to achieve an optimal match of the fluid's refractive index with that of the phantom through the use of a flow loop (Fig. 2.2) and then precisely measure the refractive index of the matching fluid using a high-precision Abbe refractometer (ATAGO NAR-3T, precision of ± 0.0001).

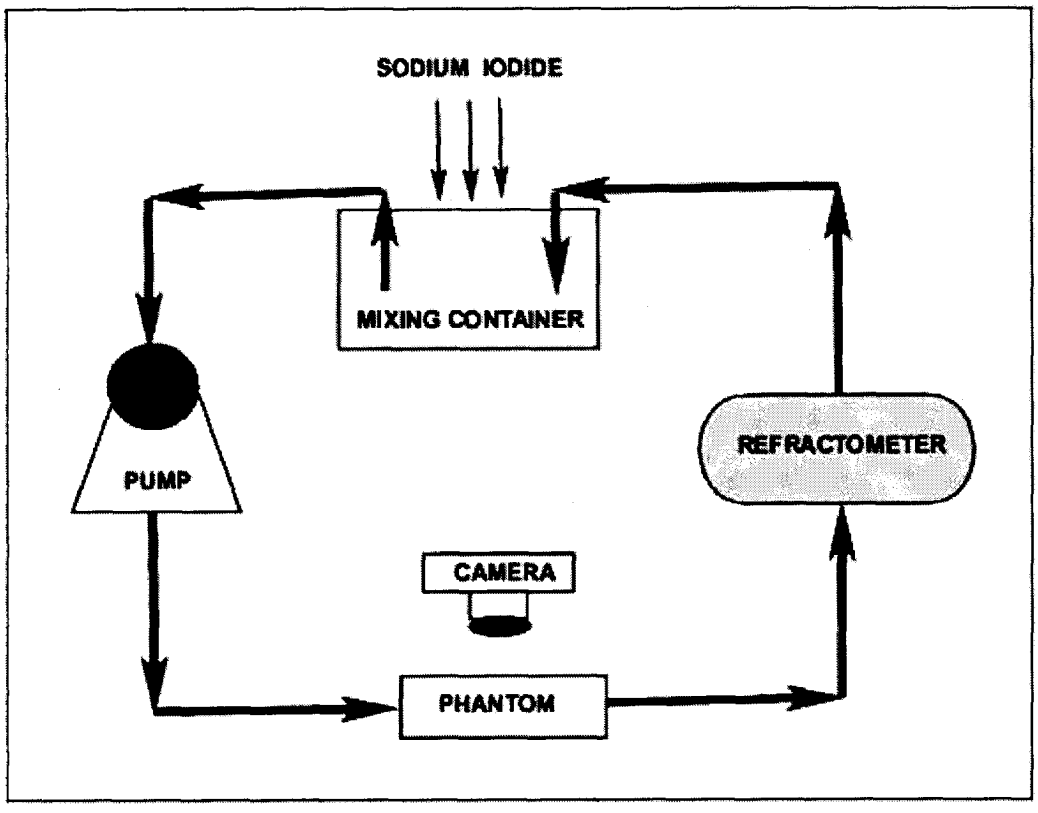

Fig. 2.2: A flow loop showing the in-line set up for simultaneous perfusion of the phantom and refractometer while monitoring the distortion of grid lines beneath the phantom due to refraction.

An initial solution was prepared with a refractive index around 1.40, which lies within the lower bound of silicone elastomers, and with an initial quantity of glycerol in water to attain a kinematic viscosity around the lower end of the range of interest. Sodium iodide salt was added in regular increments until a formulation with a refrac-

tive index matching to the specific phantom was achieved. As shown in Fig. 2.2, the fluid was mixed in a main container equipped with a magnetic stirrer. The phantom was placed over a grid paper and a peristaltic pump was used to circulate the fluid, which was adequate here since no PIV measurements were achieved (i.e. there was no need to use the computerized PIV pump here). Images were taken of the phantom using a digital camera to record the progression of the refractive-index matching process. To ensure that the temperature is consistent throughout the system, the fluid was circulated through the refractometer and then back to the mixing container. The initial fluid was composed of water (50.21% by weight), glycerol (39.14% by weight) and sodium iodide salt (10.65% by weight). This solution had a glycerol-to-water ratio of (44:56 by weight) which was held constant during the experiment. Approximate increments (0.5% by weight) of sodium iodide were weighed and added regularly while imaging the phantom for each new concentration to monitor the distortion of grid lines (Fig. 2.3). The match in refractive index was visually detected by the elimination of the distortion of grid lines, while the refractive index was precisely measured for each concentration using the Abbe refractometer. After each incremental addition of sodium iodide, approximately 30 minutes were allowed to thoroughly mix the fluid components in order to ensure accurate measurements of refractive index and assessment of distortion. After achieving the match, increments of sodium iodide were continued until the distortion of gridlines reappeared when the refractive index exceeded our match. All measurements were performed at a temperature of $22.2 \pm 0.2\,^{\circ}\mathrm{C}$.

2.2.2 Fluid refractive index and viscosity measurements

Based on our previous experimental results for the refractive index of the phantom, five fluid samples were prepared with the same initial relative concentration of glycerol-to-water (44:56 %by weight) and different concentrations of sodium iodide, in order to achieve a range of refractive index values. The range included a formulation

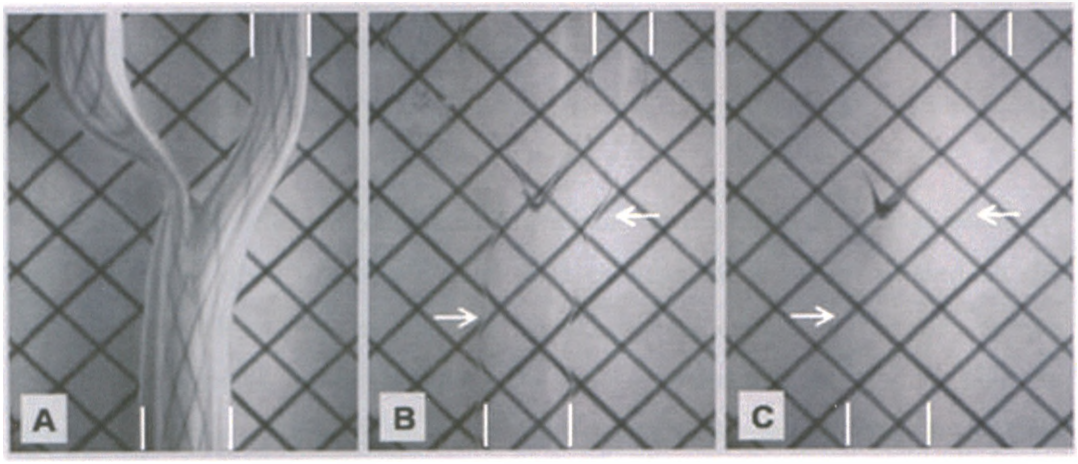

Fig. 2.3: Visual check of the refractive-index match based on monitoring the distortion of grid lines beneath a phantom filled with (A) air, showing high distortion; (B) nearly matched fluid ($n = 1.4112 \pm 0.0001$), still showing some distortion as indicated by the arrows; and (C) optimally matched fluid ($n = 1.4140 \pm 0.0001$) with no distortion, as indicated by the arrows. Note the vertical white markers, which denote the lumen, and the unintentional stain at the bifurcation apex, which also provides a convenient landmark.

with refractive index matching to our phantom, as well as four other formulations targeted to refractive index values around 1.40, 1.41, 1.42 and 1.43. For each sample, the refractive index was precisely measured using the Abbe refractometer. Kinematic viscosity was measured for each sample using a Cannon-Fenske viscometer, and density was measured using a volumetric flask and a digital scale. Dynamic viscosity (μ) was then calculated from the product of kinematic viscosity (ν) and density (ρ). Knowing that viscosity is highly dependent on glycerol, a second series of fluid samples with lower viscosity was prepared using a lower (40:60 % by weight) glycerol-to-water ratio and again with incremental sodium iodide content to achieve the desired range of refractive indices (1.40–1.43).

Note that all measurements of refractive index, viscosity, and density were repeated five times for each concentration, and then mean and standard deviation were calculated for each set of measurements. Again, all measurements in both experiments

were performed at a temperature of $22.2 \pm 0.2\,^{\circ}\mathrm{C}$.

2.2.3 Particles

Numerous particles are commercially available for use in particle image velocimetry. Typically, when selecting a particle, a compromise is required based on the particular particle parameters. Particles should be small enough so that the response time of the particles to the motion of the fluid is reasonably short which helps in following the flow accurately [5]. Note that the particle response time is the time that a particle takes to respond to a change in carrier flow velocity. Also, small diameter particles are desirable for better resolution. However, they produce less light scatter and are hence less conspicuous. To maximize reflected light, silver-coated particles can be used, but differences in density between particle and fluid may lead to settling (or floating) and thus drifting out of the illuminated region of interest (i.e. laser sheet) before reaching the end of the field of view. Calculation of a particle's terminal velocity, based on Stokes' Law for falling particles in a viscous fluid, shows that smaller sizes and smaller differences in density are thus desirable. The terminal velocity, for Stokes regime, is given by Asano *et al.* [27]:

$$V_{\infty} = \frac{(\rho_p - \rho_f) D^2 g}{18 \mu_f} \tag{2.1}$$

where V_{∞} is the particle terminal velocity (m/s), D is the particle diameter (m), g is the acceleration due to gravity (9.81 m/s^2), ρ_p is the particle density (kg/m^3), ρ_f is the fluid density (kg/m^3), and μ_f is the dynamic viscosity of the fluid in Pa·s (1 Pa·s = 1 N·s/cm^2 = 10 Poise).

Here we consider silver-coated hollow glass spheres (S-HGS-10, Dantec, New Jersey, USA), which offer excellent visibility (i.e. reflectivity) with size distribution of 2–20 μm, average size of 10 μm, and a density of 1.4 g/cm^3. Estimating a minimum fluid density of about 1.1 g/cm^3 (corresponding to 40% glycerol by volume) and thus

maximum density difference of 0.3 g/cm^3, leads to a terminal velocity of 3.7 μm/s for a 10-μm particle, with corresponding range 0.15–15 μm/s for 2–20 μm diameter range respectively. Accordingly, this would lead to a 1.5 to 150-μm drift for a conservatively long 10 s imaging time, corresponding to a loss of 0.75% to 7.5% of the 2-μm to 20-μm particles, respectively, out of the 2-mm laser sheet. For comparison, a 50-μm particle of similar density, theoretically, would drift by about 930 μm in 10 seconds or 47% of the laser sheet thickness.

Second, a flow experiment was done to provide guidance when selecting an appropriate seeding density for the selected particle. For the flow experiment, one litre of the same fluid formulation that matched our phantoms was prepared with a flow loop similar to the one used for refractive index measurements (Fig.2.2) but excluding the refractometer. The fluid was seeded with an initial concentration of 2 mg/L (corresponding to approximately 2.8 million particles/L) of S-HGS-10 particles, and gradual increments of 2–3 mg were added to the fluid until reaching a total amount of 25 mg/L. Images were taken after each increment using a high-resolution CMOS camera to visually observe the particles' reflectivity and seeding density under typical flow-study conditions. A pulsed-laser sheet of light, from a diode-pumped Nd:YAG (LSR-532-TM-5000-10, 532 nm, 5.5 W, LaserGlow.com Ltd., Toronto) laser source, was used to illuminate the particles with a 2-mm-thick laser sheet diverging across the 10-cm wide phantom and pulsing with exposure duration of 150 μs.

2.3 Results

2.3.1 Refractive index measurement of the phantom

Fig. 2.3C shows the match of refractive index between the newly developed fluid and the phantom, which was visually confirmed by the elimination of apparent distortion of grid lines beneath the phantom. The minor distortion still visible in Fig.

2.3B, with a fluid of refractive index of 1.4112±0.0001, was gradually eliminated with additional sodium iodide; the distortion was no longer visually discernible, as demonstrated in Fig. 2.3C, for a range of fluid refractive indices from 1.4132 to 1.4148, as measured coincidentally with the Abbe refractometer. Thus the refractive index of the Sylgard 184 phantom was indirectly determined to be 1.4140±0.0008, with a range corresponding to approximately ±0.5% (by weight) of sodium iodide. An optimally matched fluid, with a corresponding refractive index of 1.4140±0.0001 as measured with the Abbe refractometer, was composed of 47.38% (by weight) water, 36.94% (by weight) glycerol, and 15.68% (by weight) sodium iodide salt. Each measured value of the kinematic viscosity was multiplied by the average fluid density (1.244 ± 0.002 g/mL) to obtain corresponding dynamic viscosity values, giving an average of 4.31 ± 0.03 cP, which lies within 2.0% of the target range of human blood viscosity (4.4±0.5 cP) given in Table 1.1.

2.3.2 Fluid viscosity and refractive index measurements

Figure 2.4 shows the refractive index and dynamic viscosity, each as a function of sodium iodide concentration for the first series of fluid with a fixed glycerol-to-water ratio of 44:56 (% by weight). The refractive index was found to vary linearly ($n = 0.0017x + 1.3877$) with the sodium iodide concentration (represented by x, in percentage by weight), whereas dynamic viscosity was found to vary according to a second order polynomial fit given by $\mu = 0.0007x^2 + 0.007x + 4.0808$. As shown in Fig. 2.4 for the 44:56 glycerol-to-water solution, a range from 7 to 31% (by weight) of added sodium iodide produces refractive index values from 1.40 to 1.44 (by extrapolation) with corresponding dynamic viscosity from 4.16 to 4.96 cP. This full range of viscosity values are within an acceptable range to match human blood (±1 standard deviation), therefore this formulation simultaneously provides acceptable viscosity values for all common silicone elastomers ($n = 1.40$–1.44).

Additionally, a different combination of refractive index and dynamic viscosity

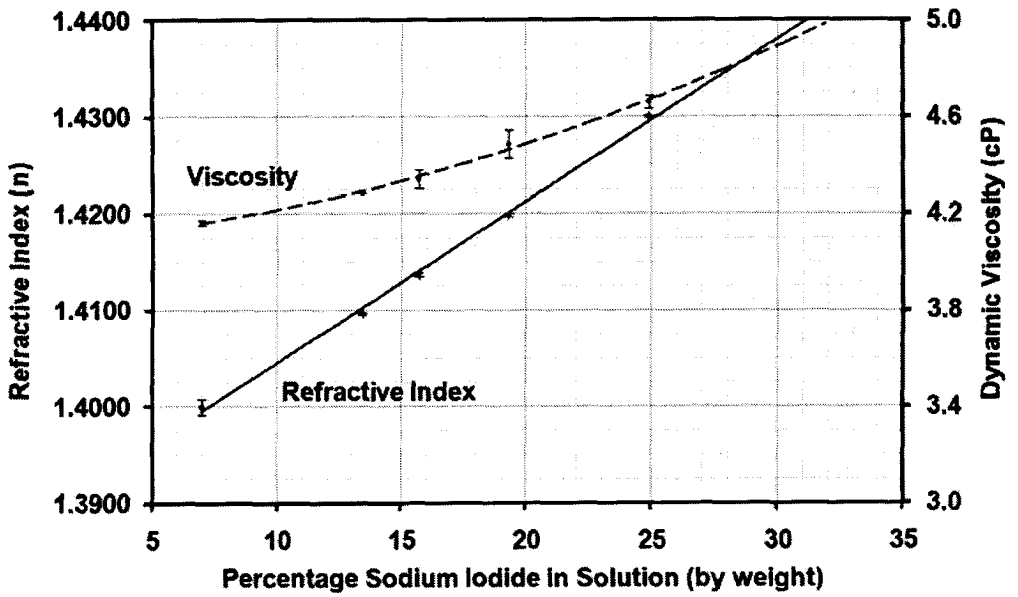

Fig. 2.4: Refractive index and viscosity each shown as a function of sodium iodide concentration in a 44:56 (% by weight) glycerol-water solution. Error bars represent standard deviation based on 5 repeated measurements.

can be obtained through a different ratio of glycerol, water, and sodium iodide, as demonstrated in Fig. 2.5, which shows the dynamic viscosity for two series of samples as a function of percentage sodium iodide, with corresponding refractive index values (with maximum uncertainty ± 0.002) shown as data labels.

The top series represents a 44:56 glycerol-to-water ratio, which has five data points with corresponding refractive indices varying from 1.400 to 1.430 that include our optimal fluid ($n = 1.4140$). The bottom series includes seven samples with 40:60 glycerol-to-water ratio and similar range of refractive index ($n = 1.404$–1.429) as the top series, where again refractive index was found to vary linearly with sodium iodide concentration ($n = 0.0018x + 1.3804$). As expected, a higher ratio of glycerol-to-water demonstrates higher viscosity, due to the fact that the viscosity of glycerol (1490 cP at 20 °C) is a thousand times higher than that of water (1.002 cP at 20 °C) [28].

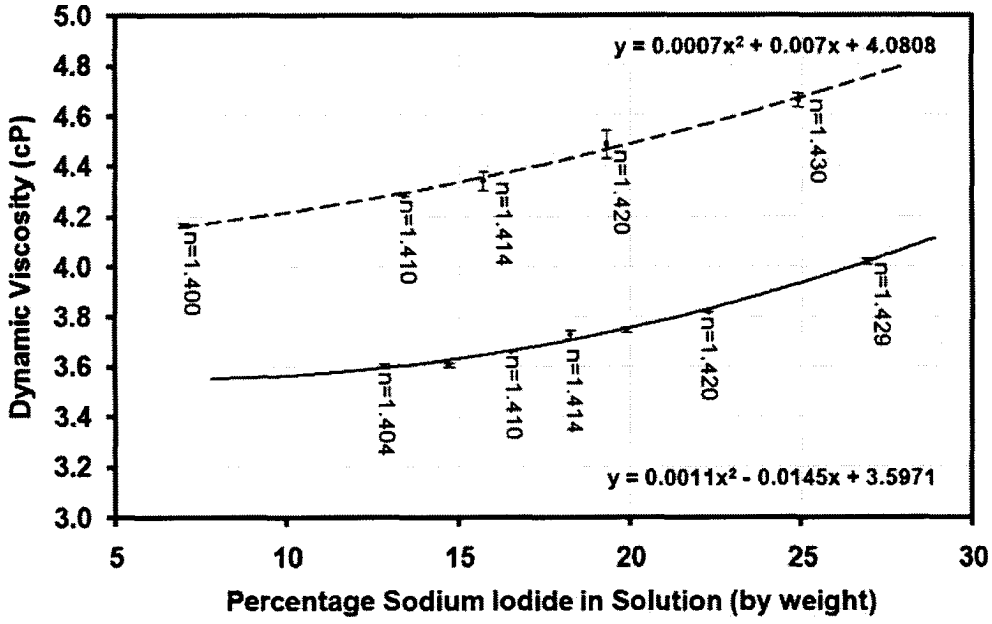

Fig. 2.5: Dynamic viscosity for two series of different (% by weight) glycerol-to-water ratios (44:56 top and 40:60 bottom), as a function of percentage sodium iodide in solution, along with curves of best fit. Also shown are the corresponding refractive index (n) values as data labels. Note that the same range of refractive indices (1.40–1.43) was matched in both series. Error bars represent standard deviation based on 5 repeated measurements.

The second series of data thus allows users to interpolate between the two series in order to yield a formulation for a precise set of refractive index and dynamic viscosity. For example, in designing PIV studies for comparison with previous ultrasound flow studies using a standard ultrasound BMF [29] with dynamic viscosity of 4.1 $\pm$ 0.1 cP, a PIV BMF with targeted refractive index of 1.4140 and dynamic viscosity of 4.1 cP should be formulated with a glycerol-water ratio of about 42.5:57.5 and 16.5% (by weight) sodium iodide, assuming linear interpolation between the two curves, for simplicity.

Fig. 2.6 shows the kinematic viscosity of the two fluid series as a function of sodium iodide concentration in solution. It demonstrates that the kinematic viscosity

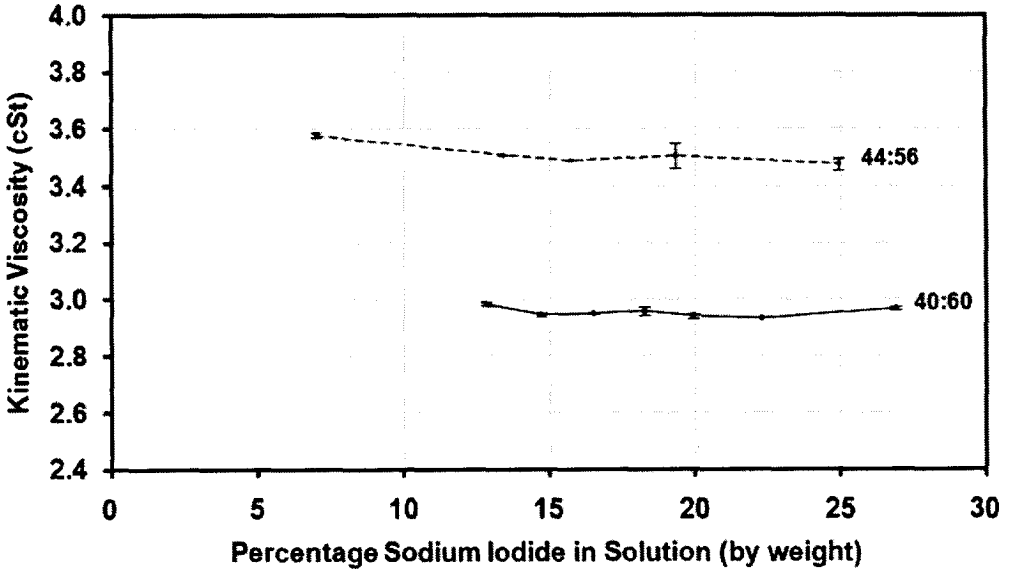

Fig. 2.6: Kinematic viscosity for different glycerol-to-water ratios (44:56 top and 40:60 bottom), as a function of sodium iodide concentration in solution, which shows that kinematic viscosity is not significantly dependent on sodium iodide concentration and mainly dependent on the relative glycerol concentration. Error bars represent standard deviation based on 5 repeated measurements.

is relatively independent of sodium iodide concentration and primarily dependent on the glycerol-to-water ratio. However, the sodium iodide salt expectantly increases the fluid density and thus also the dynamic viscosity (product of kinematic viscosity and density), as demonstrated in Fig. 2.5.

Also, the fluid formulation that achieved a match of refractive index with our Sylgard-184 phantom at $22.2 \pm 0.2\,^{\circ}\mathrm{C}$, was tested at a range of working temperatures ($20 - 25\,^{\circ}\mathrm{C}$). The resulting refractive index values for $20\,^{\circ}\mathrm{C}$ to $25\,^{\circ}\mathrm{C}$ were between 1.4138 and 1.4132 respectively, which still lie within the matching range for our phantom (1.4140±0.0008), as shown in this work. A linear fit between refractive index (n) and temperature (T) was found with n = -0.0001 T + 1.416 (R^2=0.9755). As for the dynamic viscosity (μ), a second degree polynomial fit was found with μ =

0.0041 T^2 - 0.3317 T + 9.6533 (R^2=0.998). The corresponding viscosity values were between 4.67 cP and 3.90 cP for 20 °C and 25 °C respectively, which still lie within the acceptable range for human blood viscosity (4.4 ± 0.5 cP).

Finally, Fig. 2.7 shows a series of images, corresponding to particle-seeding densities ranging from 2 to 25 mg/L, of the silver-coated, hollow-glass spheres illuminated by an approximately 2-mm thick 5.5W laser sheet. The grid paper provides 5-mm scale for determining the resulting approximate number of particles per cubic centimeter observable with the given laser parameters. Nominally, the above seeding densities should result in approximately 3,000 to 30,000 particles/cm^3 and thus 600 to 6,000 particles per square centimeter field of view for a 2-mm thick laser sheet. However, clearly fewer particles are actually visible. The smaller sized particles may not be visible due to low light scatter, while the largest scatterers seen may actually correspond to clumps of individual particles.

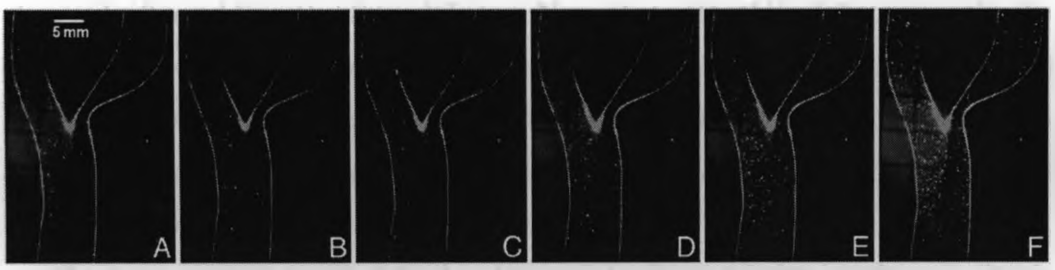

Fig. 2.7: Particle images to demonstrate particle seeding density and reflectivity when using 10-μm silver-coated hollow glass spheres (Dantec S-HGS-10) with (A) 2 mg/L, (B) 5 mg/L, (C) 10 mg/L, (D) 15 mg/L, (E) 20 mg/L, and (F) 25 mg/L. Note that the undistorted grid lines beneath the left half of the phantom show the optimal match of refractive index between the fluid and the phantom and provide a scale (5 mm^2) for determining the resulting detectable seeding density for 2-mm thick laser sheet.

Additionally, particles near the edge of the laser sheet may have insufficient light illumination. All of these factors act to reduce the number of visible particles thus indicating that over seeding is necessary to achieve sufficient density of visible scatterers.

2.4 Discussion

The described blood-mimicking fluid is safe, relatively inexpensive (approximate cost of $20/L), transparent, and colorless. The fluid did not demonstrate significant volatility and evaporation rate over a period of three days, unlike alcohol-based fluids. Finally, all measurements in this work were performed at a temperature of $22.2 \pm 0.2\,^{\circ}C$, which is ideal as it eliminates the need for temperature-control systems.

One limitation to be noted is that the fluid exhibits a discoloration (yellowing) over time, reportedly caused by the ionization of sodium iodide (releasing of I^{3-} ion) after exposure to air or light for several hours [30]. This problem can be treated by adding 0.1% (by weight) of sodium thiosulphate ($Na_2S_2O_3$) [30] to retrieve the original colorless form of the fluid. No effect on refractive index or viscosity was observed after adding the thiosulphate. Note that, the thiosulphate can also be added to the basic components when preparing the fluid to essentially prevent the ionization problem. Additionally, it should also be noted that the high concentration of sodium iodide salt can be corrosive to metal parts, and hence it is recommended to rinse or flush any flow-system components after use.

The very accurate match of fluid and material refractive index, produces an ironic limitation as it leads to a completely invisible lumen boundary which can be problematic when trying to set up an experiment. This problem may be alleviated by introducing air bubbles, which can be purged later, or by incidental landmarks in the phantom material (such as the stain seen in Fig. 2.3).

Finally, the target of this work was the best possible match of refractive index between the fluid and the phantom based on the visual match, which might be more than sufficient. In other words, the match of refractive index achieved in this work was within ± 0.0008 which corresponds to a worst case displacement, due to refraction, of

0.008 mm in the particle location based on an average angle of incidence of 45° and a maximum path length of 8 mm across the CCA diameter, which is much less than one pixel for our field of view. Such high accuracy is more than sufficient since the particle is usually given enough time to move at least 3-4 pixels between each two consecutive images in PIV.

2.5 Conclusion

A blood-mimicking fluid (BMF) composed of water, glycerol, and sodium iodide was developed in this work with a refractive index matching to commonly used castable silicone elastomers and corresponding dynamic viscosity values within an acceptable range for modeling human blood, with both parameters attained simultaneously at room temperature.

We have described a technique for the indirect measurement of the phantom's refractive index and for optimally fine tuning a formulation to accurately match the refractive index of a given phantom. This enabled us to determine the apparent refractive index of our solid Sylgard-184 phantom to be 1.4140±0.0008, whereas literature sources specify a range of 1.41–1.43 [1, 10] for the same material. This demonstrates common variability in refractive index, and thus the possible need to adjust the formulation to match each individual phantom, while maintaining consistent viscosity.

Characterization of the refractive index and viscosity as functions of sodium iodide concentration enables the adjustment of the refractive index to match different phantoms (i.e. to accommodate different materials or batch-to-batch variance in the refractive index of a given material) while attaining a reasonable dynamic viscosity for modeling blood. Further characterization of the fluid as a function of glycerol-to-water ratio enables more precisely targeting both a specific refractive index and dynamic viscosity. Consequently the three-component BMF demonstrates high versatility to cover a wide range of refractive index with simultaneous desired viscosity.

In addition, the fluid meets all desired criteria for a good PIV fluid such as optical clarity, good availability, low cost, and low user risk.

References

[1] L. M. Hopkins, J. T. Kelly, A. S. Wexler, and A. K. Prasad, "Particle image velocimetry measurements in complex geometries", *Experiments in Fluids*, vol. 29, pp. 91–95, 2000.

[2] T. T. Nguyen, Y. Biadillah, R. Mongrain, J. Brunette, J.-C. Tardif, and O. F. Bertrand, "A method for matching the refractive index and kinematic viscosity of a blood analog for flow visualization in hydraulic cardiovascular models", *Journal of Biomechanical Engineering*, vol. 126, pp. 529–535, 2004.

[3] P. Miller, K. Danielson, G. Moody, A. Slifka, E. Drexler, and J. Hertzberg, "Matching index of refraction using a diethyl phthalate/ethanol solution for in vitro cardiovascular models", *Experiments in Fluids*, vol. 41, pp. 375–381, 2006.

[4] R. Yip, R. Mongrain, A. Ranga, J. Brunette, and R. Cartier, "Development of anatomically correct mock-ups of the aorta for PIV investigations", *Canadian Design Engineering Network CDEN Conference*, Montreal 2004.

[5] Wapedia, "Particle image velocimetry ",
http : *//wapedia.mobi/en/Particle*$_i$*mage*$_v$*elocimetry*

[6] K. Nishino, and J.-W. Choi, "Index-matching PIV for complex flow geometry", *4th Japan-Korea Joint Seminar on Particle Image Velocimetry*, Kobe, Japan, 2006.

[7] R. F. Smith and D. W. Holdsworth, "Geometric characterization of stenosed human carotid arteries", *Academic Radiology*, vol. 3, pp. 898, 1996.

[8] T. L. Poepping, H. N. Nikolov, M. L. Thorne, and D. W. Holdsworth, "A thin-walled carotid vessel phantom for Doppler ultrasound flow studies", *Ultrasound Med Biol*, vol. 30, pp. 1067–1078, 2004.

[9] R. F. Smith, B. K. Rutt, and D. W. Holdsworth, "Anthropomorphic carotid bifurcation phantom for MRI applications", *J Magn Reson Imaging*, vol. 10, pp. 533–544, 1999.

[10] P. Peterka, I. Kak, V. Matejec, J. Kanka, M. Karsek, M. Hayer and J. Slnicka, "Novel coupling element for end-pumping of double-clad fibres", *ECOC.*, We4.P.127, pp. 25–29, 2006.

[11] W. L. Lim, Y. T. Chew, T. C. Chew, and H. T. Low, "Pulsatile flow studies of a porcine bioprosthetic aortic valve in vitro: PIV measurements and shear-induced blood damage", *Journal of Biomechanics*, vol. 34, pp. 1417-1427, 2001.

[12] S. Raz, S. Einav, Y. Alemu, and D. Bluestein, "DPIV prediction of flow induced platelet activation-comparison to numerical predictions", *Annals of Biomedical Engineering*, DOI: 10.1007/s10439–007–9257–2, 2007.

[13] J. Brunette, R. Mongrain, J. Laurier, R. Galaz, J. C. Tardif, "3D flow study in a mildly stenotic coronary artery phantom using a whole volume PIV method", *Med Eng Phys*, vol. 30, pp.1193–1200, 2008.

[14] A. A. Fontaine, J. T. Ellis, T. M. Healy, J. Hopmeyer, and A. P. Yoganathan, "Identification of peak stresses in cardiac prostheses - A comparison of two-dimensional versus three-dimensional principal stress analyses", *ASAIO*, vol. 42, pp. 154–163, 1996.

[15] M. Grigioni, C. Daniele, G. D'Avenio, and V. Barbaro, "The influence of the leaflets' curvature on the flow field in two bileaflet prosthetic heart valves", *J Biomec*, vol. 34, pp. 613–621, 2001.

[16] J. M. Sankovic, J. R. Kadambi, M. Mehta, W. A. Smith, and M. P. Wernet, "PIV investigations of the flow field in the volute of a rotary blood pump", *Journal of Fluids Engineering-Transactions of the Asme*, vol. 126, pp. 730–744, 2004.

[17] S. Sastry, J. R. Kadambi, J. M. Sankovic and V. Izraelev, "Study of flow field in an advanced bladeless rotary blood pump using Particle Image Velocimetry", *In: 13th Int Symp on Appl Laser Techniques to Fluid Mechanics*, Lisbon, Portugal, 2006.

[18] T. Yagi, W. Yang, D. Ishikawa, H. Sudol, K. Iwasaki, and M. Umezul, "Multiplane scanning stereo-PIV measurements of flow inside a spiral vortex pulsatile blood pump", *In: 13th Int Symp on Applications of Laser Techniques to Fluid Mechanics*, Lisbon, Portugal, 2006.

[19] A. Vaya, J. Murado, M. Santaolaria, M. Simo, and L. Mico, "Haemorheological changes in patients with systemic lupus erythematosus do not seem to be related to thrombotic events", *Clinical Hemorheology and Microcirculation*, vol. 38, pp. 23-29, 2008.

[20] J. C. F. Galduroz, H. K. Antunes, and R. F. Santos, "Gender- and age-related variations in blood viscosity in normal volunteers: A study of the effects of extract of Allium sativum and Ginkgo biloba", *Phytomedicine*, vol. 14, pp. 447-451, 2007.

[21] L. Carrera, R. Etchepare, M. Arrigo, S. Vaira, J. Valverde, A. D'Ottavio and P. Foresto, "Hemorheologic changes in type 2 diabetic patients with microangiopathic skin lesions. A linear discriminant categorizing analysis", *Journal of Diabetes and Its Complications*, vol. 22, pp. 132-136, 2008.

[22] M. W. Rajzer, M. Klocek, W. Wojciechowska, I. Palka and K. L. Kawecka-Jaszcz, "Relationship between, blood viscosity, shear stress and arterial stiffness in patients with arterial hypertension", *Elsevier*, 2007.

[23] M. Bor-Kucukatay, A. Keskin, H. Akdam, S. Kabukcu-Hacioglu, G. Erken, P. Atsak, and V. Kucukatay, "Effect of thrombocytapheresis on blood rheology in healthy donors: Role of nitric oxide", *Transfusion and Apheresis Science*, doi:10.1016/j.transci, 2008.

[24] M. Fehr, K. S. Galliard-Grigioni and W. H. Reinhart, "Influence of acute alcohol exposure on hemorheological parameters and platelet function in vivo and in vitro", *Clinical Hemorheology and Microcirculation* , vol. 39, pp. 351-358, 2008.

[25] N. Antonova, E. Zvetkova, I. Ivanov and Y. Savov, "Hemorheological changes and characteristic parameters derived from whole blood viscometry in chronic heroin addicts", *Clinical Hemorheology and Microcirculation* , vol. 39, pp. 53-61, 2008.

[26] P. Peterka, I. Kak, V. Matejec, J. Kanka, M. Karsek, M. Hayer and J. Slnicka, "Novel coupling element for end-pumping of double-clad fibres", *ECOC*, We4.P.127, pp. 25–29, 2005.

[27] K. Asano, "Mass transfer: from fundamentals to modern industrial applications", *Wiley-VEH*, chapter 6, pp. 107, 2006.

[28] R. C. Weast, "CRC handbook of chemistry and physics. A ready-reference book of chemical and physics data", *Chemical Rubber Company*, CRC Press, Clevelend, Ohio, USA, 1969.

[29] K. V. Ramnarine, D. K. Nassiri, P. R. Hoskins, and J. Lubbers, "Validation of a new blood-mimicking fluid for use in Doppler flow test objects", *Ultrasound in Medicine and Biology*, vol. 24, pp. 451–459, 1998.

[30] T. L. Narrow, M. Yoda, and S.I. Abdel-Khalik, "A simple model for the refractive index of sodium iodide aqueous solutions", *Experiments in Fluids*, vol. 28, pp. 282-283, 2000.

Chapter 3

Summary and Future work

3.1 Summary

The purpose of this thesis was to develop a blood-mimicking fluid (BMF) that enables achieving optical vascular flow model measurements with high accuracy. This involved the preparation of a fluid that demonstrates all the basic requirements as a typical PIV fluid, such as optical clarity, user safety, and availability, as well as particular requirements such as refractive index and dynamic viscosity.

A literature search on human blood viscosity showed a range of values (4.4 $\pm$ 0.5 cP) that is higher than the viscosity of commonly used blood-mimicking fluids (around 3.5 cP), and thus the targeted viscosity range for the new BMF developed in this work, was 4.4 $\pm$ 0.5 cP. Also, literature search results for refractive index (n) values, showed a range between 1.40–1.44 for silicone elastomers commonly used in vascular research, therefore the new BMF was designed to cover this particular range of refractive index values.

Different PIV fluids found in the literature were investigated in this study. We chose to pursue a BMF composed of different concentrations of water, glycerol, and sodium iodide. A flow-loop method was introduced in this work in order to develop the required BMF that works with vascular models fabricated from different silicone

elastomers. In the flow-loop method, a formulation starting with an initial water-to-glycerol ratio, was prepared. Sodium iodide was gradually added while testing the visual match of refractive index between the fluid and the phantom, with the help of a camera and a printed line grid beneath the phantom. The final formulation was achieved when the distortion in grid lines was eliminated, indicating the desired match of refractive index between the fluid and the phantom.

The method can be used for optimally fine tuning a formulation to accurately match the refractive index of a given phantom. In this work an optimal match for our Sylgard-184 phantom was achieved with a formulation composed of 47.38% (by weight) water, 36.94% (by weight) glycerol, and 15.68% (by weight) sodium iodide salt.

In addition, the flow-loop method enables indirect measurement of the phantom's refractive index. Accordingly, the apparent refractive index of our solid silicone (Sylgard-184) phantom was determined to be 1.4140±0.0008, although literature sources specify a range of 1.41–1.43 for the same material [1, 2].

Fluid compositions with different glycerol-to-water ratios, were prepared and characterized with respect to refractive index (n) and dynamic viscosity (μ). The two properties (n and μ) were characterized as functions of glycerol-to-water ratio and percentage of sodium iodide in solution. This will help other similar work to generate fluid formulations with the desired requirements based on the particular silicone phantoms used.

In conclusion, a fluid formulation that covers a range of refractive indices for silicone elastomers ($n = 1.40$–1.44), was developed. The corresponding dynamic viscosity values for the developed formulations were also within the targeted range of human blood. Both parameters were attained simultaneously at room temperature (22.2 ± 0.2 °C). Such simultaneous match of both refractive index and viscosity at room temperature, has not been introduced previously in vascular literature. In addition, the flow-loop method enables accurate matching of the refractive index between the

silicone elastomer model and the blood mimicking fluid, and consequently indirect determination of the refractive index of the phantom using a refractometer to measure the refractive index of the fluid. The method has a particular advantage because phantoms may have batch-to-batch differences (i.e. phantom to phantom variances even when manufactured from materials supplied by the same source), which implies the need for such an approach in order to develop an appropriate fluid that suits each individual phantom. In addition, with the help of the charts introduced in this work, a reasonable prediction of the primary amounts of fluid can be obtained. The method is described in detail in Chapter 2 which was submitted as a manuscript for publishing in the peer reviewed journal *Experiments in Fluids*, (M.Y. Yousif, *et al.*).

3.2 Future directions

The preceding thesis chapters describe the development of a blood mimicking fluid to work for PIV measurements in vascular models (phantoms) fabricated from silicone elastomers (n = 1.40–1.44). This work has the potential for further directions to be completed as part of future work.

Others might be interested in using the fluid with phantoms manufactured from materials other than silicone (i.e. with materials having refractive index values outside the range of silicone elastomers (n = 1.40–1.44)). Since this is a three-component fluid, it gives more flexibility to extend the ranges of refractive index and viscosity. For example, the refractive index can be changed by controlling the sodium iodide content, with minimal change in glycerol content and thus viscosity.

The fluid stability was not tested in this work therefore it might be a part of future work to test the stability of the newly developed fluid. In particular, the fluid can be tested for any changes in refractive index and viscosity over time and use.

Also for working with the newly developed fluid, it is necessary to test the phantom stability over time which was not tested in this work. In other words, silicone

phantoms might suffer discoloration due to sodium-iodide. Moreover, the phantom refractive index might change over time and temperature, which is not expected to be significant. However it might be helpful to test the refractive index of the phantom periodically as part of the future work.

Finally, it is important to mention that the newly developed fluid has some limitations to be considered for future work. In particular, the fluid suffers an ionization problem which causes discoloration where the fluid color is changed from colorless to yellow. In addition the fluid might have a corrosive effect on the metal parts of the hydraulic system, caused by the sodium iodide salt. Accordingly, it is important to rinse the system regularly and to avoid keeping the fluid inside the system for an extended period of time. Another limitation is the possible batch-to-batch variances of the fluid. In other words, it is important to test the refractive indices of more than one batch of the same fluid composition to check for any differences in the refractive index.

References

[1] L. M. Hopkins, J. T. Kelly, A. S. Wexler, and A. K. Prasad, "Particle image velocimetry measurements in complex geometries", *Experiments in Fluids*, vol. 29, pp. 91–95, 2000.

[2] P. Peterka, I. Kak, V. Matejec, J. Kanka, M. Karsek, M. Hayer and J. Slnicka, "Novel coupling element for end-pumping of double-clad fibres", *ECOC*, We4.P.127, pp. 25–29, 2005.

Appendix A

Copyright agreements

Chapter 2 of the thesis contains material from a manuscript that was submitted for publication with "*Experiments in Fluids*". Experiments in Fluids does not require that the author of a publication receive copyright permission for duplication of the published manuscript as part of a thesis, as stated on their copyrights information section "Submission of a manuscript implies: that the work described has not been published before (except in form of an abstract or as part of a published lecture, review or thesis)". Details available at:
http://www.springer.com/engineering/journal/348?detailsPage=copyrightInformation

Chapter 1 of the thesis contains a figure from an article in the literature, by Heise *et al.*: "*Correlation of Intimal Hyperplasia Development and Shear Stress Distribution at the Distal End-side-anastomosis, in vitro Study Using Particle Image Velocimetry*". Permission from the publisher, Elsevier Limited, was obtained in order to use this figure for the thesis chapter. A copy of the license, indicating that permission was granted to use parts of the published work in this thesis, is attached (Fig. A.1).

Order Completed

Thank you for placing your Rightslink license request for reuse of Elsevier Limited content. It consists of your order details, the terms and conditions provided by Elsevier Limited and the payment terms and conditions.

Get the printable license.

License Number	2267990985098
License date	Sep 14, 2009
Licensed content publisher	Elsevier
Licensed content publication	European Journal of Vascular and Endovascular Surgery
Licensed content title	Correlation of Intimal Hyperplasia Development and Shear Stress Distribution at the Distal End-side-anastomosis, *in vitro* Study Using Particle Image Velocimetry
Licensed content author	M. Heise, U. Krüger, R. Rückert, R. Pfitzman, P. Neuhaus and U. Settmacher
Licensed content date	October 2003
Volume number	26
Issue number	4
Pages	10
[illegible] of Use	Thesis / Dissertation
Portion	Figures/table/illustration/abstracts
Portion [illegible]	1
Format	Electronic
You are the author of this Elsevier article	No
Are you translating?	No
Order Reference Number	
Expected publication date	Sep 2009
Elsevier VAT number	GB 494 6272 12
Billing type	Invoice
[illegible]any	MAJID MY YOUSIF
Billing address	304 Physics and Astronomy
[illegible]	1150 Richmond Street
	London, ON N6A 3K7
	Canada
Customer reference info	
Permissions price	0.00 USD
Value added tax 0.0%	0.00 USD
Total	0.00 USD

ORDER MORE... CLOSE WINDOW

Fig. A.1: Licence of permission granted by Elsevier to use a figure, from a published work, in chapter 1 of this thesis. The figure was modified to produce Fig. 1.2 in this work.